Broad HOMO–LUMO gap tuning through the coordination of a single phosphine, aminophosphine or phosphite onto a Ru(tpy)(bpy)$^{2+}$ core†

Isabelle M. Dixon,[a] Emilie Lebon,[a] Gilles Loustau,[a] Pierre Sutra,[a] Laure Vendier,[a] Alain Igau*[a] and Alberto Juris[b]

Received 18th April 2008, Accepted 1st July 2008
First published as an Advance Article on the web 2nd September 2008
DOI: 10.1039/b806325g

The synthesis of new ruthenium(II) terpyridine bipyridine complexes bearing a phosphorus(III) ligand is presented. The steric and electronic properties of the phosphorus ligand were varied using aminophosphines, alkyl and aryl phosphites and the bulky tri(isopropyl)phosphine. All complexes were characterized by multi-nuclear NMR spectroscopy, mass spectrometry and X-ray diffraction analysis. The electronic properties of the complexes were probed by cyclic voltammetry, absorption and luminescence spectroscopy. The complexes do not show luminescence at room temperature, whereas at 77 K in an alcoholic matrix, emission is observed in the range 600–650 nm with lifetimes of 3.5–5.5 μs, originating from ^{3}MLCT states. The MLCT transition spans over 65 nm, which corresponds to a variation of 0.4 eV in the HOMO–LUMO gap. The oxidation potential of the ruthenium varies over a broad range of 290 mV, from +1.32 V *vs.* SCE with L = P^{i}Pr$_3$ to +1.61 V *vs.* SCE with L = P(OPh)$_3$. This range is unprecedented upon the variation of a single monodentate ligand coordinated by the same heteroatom in the same oxidation and charge states. This work underlines the specific capacity of phosphorus in bringing up a large variety of electronic properties by changing its substituents.

Introduction

Progress in solar energy conversion technology is a major challenge for sustainable development.[1] This interdisciplinary field of research is at the crossroads between material science, polymer science, molecular chemistry and physics, as illustrated by the variety of journals publishing reports in this field.[2] Among all types of solar energy conversion devices, dye-sensitized solar cells (DSSC) seem to be the best compromise in terms of ease of preparation, cost and efficiency.[3] This research was initiated by the pioneering work of Grätzel and his group,[4] which has greatly contributed to the development of many families of ruthenium dyes in the past 15 years.[5] Much of the current research in this field aims at improving the electrolyte[6] and the semiconductor,[7] but the increase of the performance of dye-sensitized solar energy conversion devices also relies on the development of new families of dye complexes.[8] In the context of the development of new complexes for DSSC, we started fundamental studies on ruthenium terpyridine bipyridine complexes bearing one monodentate phosphorus-based ligand,[9] surprisingly neglected in the literature. There is indeed only one example of a Ru(tpy)(bpy)$^{2+}$ complex bearing a phosphorus ligand of the triphenylphosphine type.[10] Phosphorus is nevertheless a widely used coordinating heteroatom the electronic[11] and steric[12] properties of which can be tremendously altered by changing its substituents and oxidation state. Neutral phosphorus(III) ligands of various σ and π abilities were coordinated on Ru(tpy)(bpy)$^{2+}$ to probe the limits of the accessible redox range and to pave the way for future work. In addition to phosphines, various types of P(III) ligands such as aminophosphines and phosphites were selected in order to cover a wider range of electronic properties, in particular the HOMO–LUMO gap as reflected by the energy of the MLCT (metal-to-ligand charge transfer) transition. The electronic properties of the complexes have been studied by UV-visible absorption spectroscopy, luminescence studies and electrochemistry.

Results and discussion

Selection of the ligands

The donor and acceptor properties of P(III) compounds are easily tuned by changing the nature of the substituents on the phosphorus atom. Pyrrolyldiphenylphosphine **1** was chosen for its π-acceptor properties,[13] while pyrrolidinyldiphenylphosphine **2** has powerful σ-donating properties.[14] In addition, the π-accepting properties of phosphites vary according to the substituents on the oxygen atoms of P(OR)$_3$, and are gradually increased on going from alkylphosphites[15] **3–5** to arylphosphites **6**.[16] Tri(isopropyl)phosphine **7** was coordinated to complement our data on ruthenium phosphine complexes,[9] and as a steric probe for future developments of this work.

[a]*Laboratoire de Chimie de Coordination du CNRS, UPR 8241, 205 route de Narbonne, 31077 Toulouse Cedex 4, France. E-mail: alain.igau@lcc-toulouse.fr; Fax: +33 561 553 003; Tel: +33 561 333 159*
[b]*Dipartimento di Chimica "G. Ciamician", Università di Bologna, via Selmi 2, 40126 Bologna, Italy. E-mail: alberto.juris@unibo.it; Fax: +39 512 099 456; Tel: +39 512 099 481*

† Electronic supplementary information (ESI) available: Cyclic voltammograms of complexes [Ru]**1**–[Ru]**9**. Absorption and emission spectra of complexes [Ru]**1**–[Ru]**9**. CCDC reference numbers 665729 (compound **1**·BH$_3$), 665730 (compound **2**·Se) and 665731–665737 (complexes [Ru]**1**–[Ru]**7**). For ESI and crystallographic data in CIF or other electronic format see DOI: 10.1039/b806325g

Synthesis of compounds 1, 1·BH_3, 2 and 2·Se

Ligands **1** and **2** were synthesized according to the literature by reacting two equivalents of amine with chlorodiphenylphosphine.[17] X-Ray quality crystals were obtained for **1**·BH_3, prepared by reacting **1** and BH_3·THF in CH_2Cl_2,[18] by evaporation of an Et_2O solution of the compound. **1**·BH_3 crystallizes in the triclinic $P\bar{1}$ space group (Fig. 1), with a P–B bond length of 1.910(5) Å, in the range of those reported for other aminophosphine boranes.[19] The asymmetric unit is composed of two molecules but only one set of bond lengths and bond angles is reported since they are similar in both molecules (Table 1). The selenide derivative of **2** was prepared by refluxing it with elemental selenium in toluene, and single crystals of **2**·Se were obtained by the slow evaporation of a toluene solution of the compound (Fig. 1). The P–Se bond length (2.1049(8) Å) is in the same range as those reported for aminophosphine selenides.[20]

Coordination on the Ru(tpy)(bpy)$^{2+}$ core

The coordination of a monodentate phosphorus ligand **1–9** on the Ru(tpy)(bpy)$(PF_6)_2$ fragment (abbreviated [Ru]) takes place in the presence of a ten-fold excess of ligand with respect to the precursor complex [Ru]$NCCH_3$,[21] under photolabilization conditions.[22] After irradiation of the solution in acetone by a 300 W halogen lamp in a closed Schlenk tube under autogenous pressure, the reaction mixture is precipitated in 20 volumes of diethylether to eliminate excess ligand and other neutral species in the supernatant. The solid hereafter obtained is purified by column chromatography on silica gel. In a final step, the nitrate counter ions are replaced by hexafluorophosphates to ensure solubility in organic solvents. Complexes [Ru]**1**–[Ru]**9** are shown in Scheme 1.

Table 1 Selected crystallographic data, collection parameters, bond lengths and bond angles for compounds **1**·BH_3 and **2**·Se

Compound	**1**·BH_3	**2**·Se
Formula	$C_{16}H_{17}BNP$	$C_{16}H_{18}NPSe$
FW	265.09	334.24
T	150 K	160 K
Space group	$P\bar{1}$	$P2_1/n$
a/Å	9.503(2)	9.0551(15)
b/Å	10.494(2)	17.944(4)
c/Å	15.347(3)	9.1410(8)
α/°	90.182(15)	90
β/°	99.474(16)	97.767(10)
γ/°	103.301(18)	90
V/Å^3	1467.7(5)	1471.7(4)
Z	4	4
ρ_{calcd}	1.200	1.509
θ range/°	3.08–25.68	2.54–32.31
μ/mm^{-1}	0.172	2.646
Reflections collected	10 776	14 968
Unique reflections	5575	4970
R_{int}	0.0750	0.0914
Refinement method	Refined on F^2	Refined on F^2
Data/parameters	5575/345	4970/172
Goodness of fit	0.915	1.020
R_1 ($I>2\sigma(I)$)	6.61%	4.84%
wR_2 ($I>2\sigma(I)$)	14.47%	13.00%
$\Delta\rho_{min}/\Delta\rho_{max}$/e Å^{-3}	0.895/–0.387	1.047/–0.888
Selected bond lengths/Å		
P1–C5	1.793(4)	P1–C5 1.807(3)
P1–C11	1.777(4)	P1–C11 1.807(3)
P1–N1	1.729(4)	P1–N1 1.642(3)
P1–B1	1.910(5)	P1–Se1 2.1049(8)
Selected bond angles/°		
C5–P1–C11	106.63(18)	C5–P1–C11 105.40(13)
C5–P1–N1	103.80(17)	C5–P1–N1 104.12(13)
C11–P1–N1	105.32(18)	C11–P1–N1 103.99(13)
N1–P1–B1	112.8(2)	N1–P1–Se1 116.43(9)

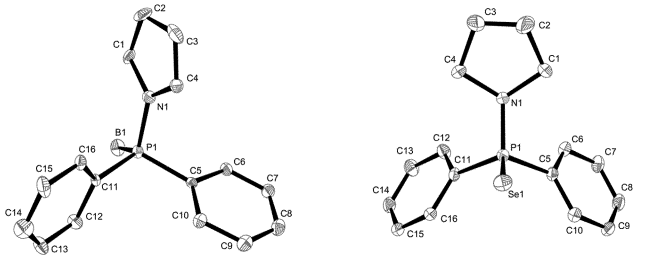

Fig. 1 ORTEP representation of compounds **1**·BH_3 and **2**·Se with 30% probability displacement ellipsoids. Hydrogen atoms are omitted for clarity.

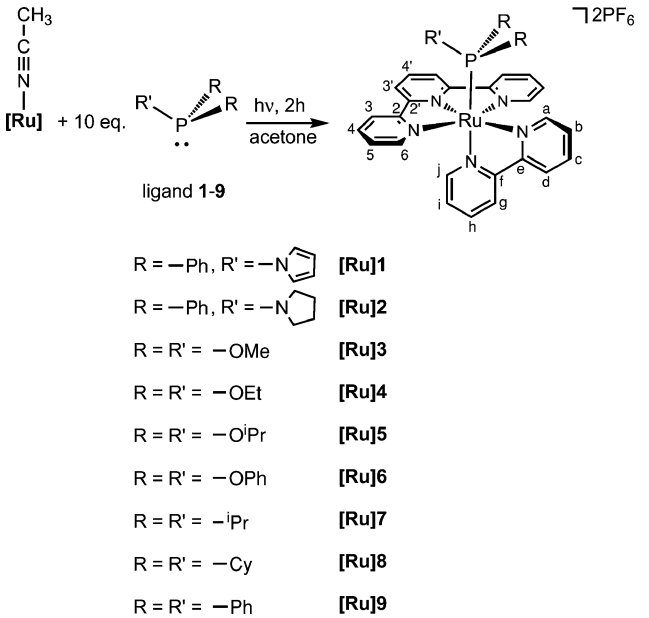

Scheme 1 The coordination of P(III) ligands **1–9** onto a Ru(tpy)(bpy)$^{2+}$ core and NMR labelling scheme.

Under the conditions used for the coordination of the ruthenium fragment, tris(amino)phosphines $P(NMe_2)_3$ and $P(NEt_2)_3$ decomposed into a multitude of phosphorus compounds as judged by ^{31}P NMR and hence, they could not be coordinated.

Characterizations

All complexes were fully characterized by ^{1}H, ^{13}C and ^{31}P NMR spectroscopy, mass spectrometry and X-ray diffraction on mono crystals. The complete assignment of ^{1}H and ^{13}C NMR signals was enabled by 2D NMR experiments. Similarly to what was described earlier for [Ru(tpy)(bpy)L]$^{2+}$ type complexes,[10,23] we found that the H_a proton on the bpy moiety, pointing towards the sixth

Table 2 NMR chemical shifts of the complexes in d_6-acetone

Complex	[Ru]**1**	[Ru]**2**	[Ru]**3**	[Ru]**4**	[Ru]**5**	[Ru]**6**	[Ru]**7**	[Ru]**8**[a]	[Ru]**9**[a]
δ ^1H_a/ppm	9.39	10.23	9.93	9.95	9.91	10.38	9.87	9.78	9.50
J (H_a–H_b)/Hz	6.0	6.0	5.4	5.7	5.4	5.7	5.7	5.4	5.7
δ ^{31}P/ppm	92.2	78.1	126.3	121.6	118.3	115.4	30.0	22.7	39.8

[a] From ref. 12.

monodentate ligand of the complex (Scheme 1), is sensitive to the nature of this latter ligand. Thus, in most cases, its chemical shift can be used as a probe to monitor the substitution of the acetonitrile molecule of the precursor complex, whose H_a appears as a doublet with $\delta = 9.93$ ppm ($J = 5.6$ Hz) in d_6-acetone (Table 2).

The ^{31}P NMR spectra of the complexes gave two signals, one corresponding to the coordinated phosphorus ligand, and a heptuplet, which corresponds to the presence of hexafluorophosphate counter ions in the region of −144 ppm ($708 < J_{PF} < 712$ Hz).

The seven crystallographic structures (Fig. 2 and Table 3) share the same relatively disordered hexafluorophosphate counter ions, and some of the structures having their diffracted intensities recorded at 100 K. The Ru–P bond length (Table 4) varies significantly from 2.2268(11)–2.4376(9) Å, but poorly correlates with the Tolman cone angle of the ligand (not shown),[12] showing the interplay between the global electronic and steric effects of the substituents on the phosphorus atom and their direct influence upon the net donor power of the coordinating atom:[24] π-Accepting phosphites result in the shortest Ru–P bond lengths (2.22–2.26 Å), intermediate aminophosphines give rise to Ru–P bonds of medium lengths (2.31–2.35 Å), and phosphines yield the longest Ru–P bond lengths (2.35–2.44 Å).[9] In the case of the aminophosphine ligands, the Ru–P bond is longer in [Ru]**2** than in [Ru]**1** as a result of both electronic and steric effects. Indeed the N6 nitrogen atom is planar in [Ru]**1** (sum of angles at N6 = 359°) while it is more pyramidal and hence more bulky in [Ru]**2** (sum of angles at N6 = 349 °). This compares well with what was found in the adduct **1**·BH_3 (sum of angles 359.8°) and compound **2**·Se (sum of angles 344.3°), in which the nitrogen lone pair points *trans* to the phosphorus–selenium bond. On the other hand, taking into account the esd's, the length of the Ru–N1 bond *trans* to the Ru–P bond varies only slightly, which indicates that the electronic effects of the sixth ligand mostly focus within the Ru–P bond. An intramolecular stacking interaction in complex [Ru]**2** (inter-plane distance d = 3.06 Å, offset angle α = 34°) could account for the different orientation of the phenyl substituents on the phosphorus, although the offset angle is relatively large.[25] Besides, a close examination of the structure of complex [Ru]**6** shows a strong distortion of the terpyridine ligand. The dihedral angles between the peripheral pyridine rings and the central pyridine ring are 12.9 and 15.3°. Upon looking at the X-ray structure one can clearly not invoke steric hindrance to account for such a distortion. This is consistent with the fact that the cone angle of triphenylphosphite is 128°, and steric effects are expected to be relatively small.[12] Crystal packing forces, however, are evidenced by a series of π–π stacking interactions (inter-plane distance d = 3.65 Å, offset angle $\alpha = 26°$, and d = 3.75 Å, $\alpha = 19°$), which are also found intramolecularly (d = 3.43 Å, $\alpha = 7°$ and d = 3.36 Å, $\alpha = 30$ °). (Fig. 3).[25]

Discussion

The main challenge in ruthenium polypyridine chemistry lies in the ability to customize the net donating properties of the ancillary ligand(s) in order to modulate the Ru^{III}/Ru^{II} potential and the energy

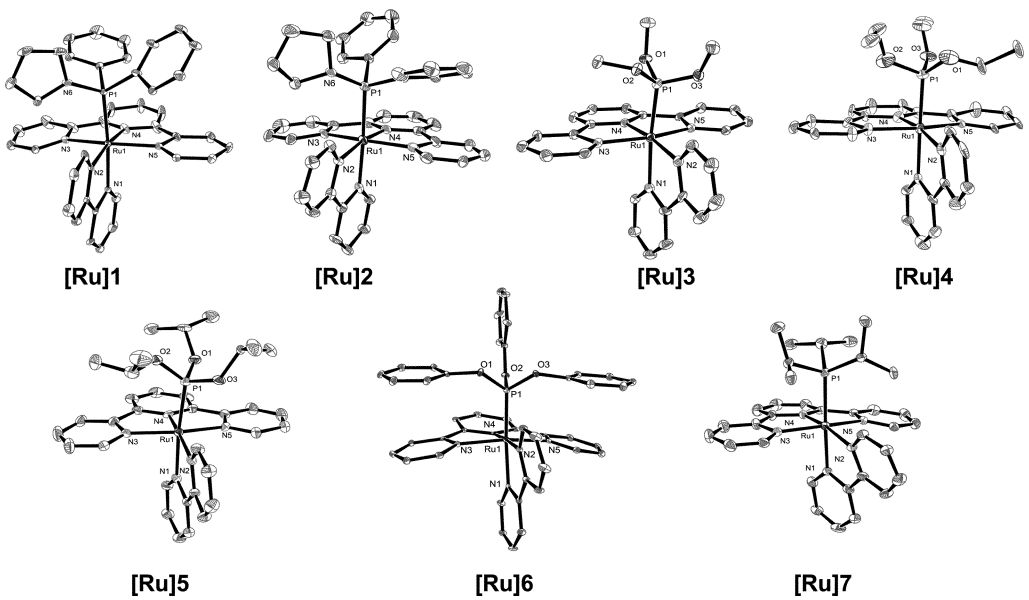

Fig. 2 ORTEP view of complexes [Ru]**1**–[Ru]**7** with 30% probability displacement ellipsoids. Solvent molecules, hydrogen atoms and anions are omitted for clarity.

Table 3 Selected crystallographic data and collection parameters for complexes [Ru]**1**–[Ru]**7**

Complex	[Ru]**1**	[Ru]**2**	[Ru]**3**	[Ru]**4**	[Ru]**5**	[Ru]**6**	[Ru]**7**
Formula	$C_{41}H_{33}N_6PRu{\cdot}P_2F_{12}{\cdot}C_3H_6O$	$C_{41}H_{37}N_6PRu{\cdot}P_2F_{12}$	$C_{28}H_{28}N_5O_3PRu{\cdot}P_2F_{12}{\cdot}C_3H_6O$	$C_{31}H_{34}N_5O_3PRu{\cdot}P_2F_{12}$	$C_{34}H_{40}N_5O_3PRu{\cdot}P_2F_{12}{\cdot}2(C_3H_6O)$	$C_{43}H_{34}N_5O_3PRu{\cdot}P_2F_{12}$	$C_{34}H_{40}N_5PRu{\cdot}P_2F_{12}$
FW	1089.79	1035.76	962.61	946.61	1104.85	1090.73	940.69
Colour	Red–orange	Red–orange	Red–orange	Yellow–orange	Red–orange	Yellow–orange	Red
T/K	103	180	100	100	180	100	150
Space group	$P\bar{1}$	$P2_1/n$	Cc	$Pbca$	$Pna2_1$	$Pbca$	$P\bar{1}$
a/Å	9.6647(4)	17.7785(16)	22.058(3)	20.5612(6)	22.5924(9)	14.609(3)	14.9512(9)
b/Å	11.7577(5)	19.299(2)	16.561(3)	14.9833(5)	13.7879(7)	14.272(3)	15.1059(10)
c/Å	22.6217(10)	14.1272(12)	12.834(2)	29.1467(7)	15.3670(7)	39.990(8)	20.1824(14)
α/°	76.051(4)	90	90	90	90	90	103.205(6)
β/°	85.002(4)	91.932(11)	126.380(19)	90	90	90	97.589(5)
γ/°	76.882(4)	90	90	90	90	90	102.186(5)
V/Å^3	2428.27(18)	4844.5(8)	3774.6(14)	8979.4(5)	4786.8(4)	8338(3)	4259.1(5)
Z	2	4	4	8	4	8	4
ρ_{calcd}/g cm^{-3}	1.490	1.420	1.694	1.400	1.533	1.738	1.467
θ range/°	2.80–24.71	2.10–26.02	4.61–26.37	2.72–25.03	3.08–25.68	2.85–26.37	2.87–25.35
μ/mm^{-1}	0.508	0.504	0.646	0.540	0.522	0.595	0.564
Reflections collected/unique	14 809/8215	47 479/9479	12 578/6488	59 297/7915	33 474/8910	52 199/8501	30391/15 520
R_{int}	0.0343	0.0010	0.0366	0.1081	0.0580	0.1123	0.0765
Refinement method	Refined on F^2	Refined on F	Refined on F^2	Refined on F^2	Refined on F^2	Refined on F^2	Refined on F^2
Data/parameters	8215/570	3531/577	6488/510	7915/500	8910/622	8501/604	15 520/933
Goodness of fit	1.080	1.116	1.003	0.959	1.025	0.950	1.017
R_1 ($I>2\sigma(I)$)	8.06%	6.00%	3.84%	6.63%	4.85%	4.84%	8.42%
wR_2 ($I>2\sigma(I)$)	23.67%	6.90%	8.08%	17.27%	12.81%	4.96%	23.26%
$\Delta\rho_{min}/\Delta\rho_{max}$/e Å^{-3}	3.148/−1.852	0.67/−0.90	0.628/−0.395	1.386/−0.800	0.798/−0.743	0.608/−0.389	1.726/−1.275

Fig. 3 Stacking interactions in the elementary motif of the crystallized complex [Ru]**6**.

of the MLCT transition. In the case of the phosphorus ligands, ^{31}P NMR spectroscopy of the corresponding selenide is a simple and powerful tool to estimate the electronic properties of the parent ligand, with the P–Se coupling constant illustrating the basicity of the phosphorus atom,[26] with little steric bias.[27] Phosphorus(III) compounds with strong σ-donating properties give rise to a small $^1J_{PSe}$, due to the limited s-character of the phosphorus lone pair. The phosphine selenides and selenophosphates were prepared according to the literature.[17] As expected, the aminophosphines **1–2** show an intermediate basicity (J_{PSe} ~ 800 Hz) between the phosphines (J_{PSe} ~ 700 Hz) and the phosphites (J_{PSe} > 900 Hz).[28–30] Triphenylphosphite is the weakest σ-donating ligand and has a coupling constant of 1039 Hz with selenium (Table 5).

All of the complexes [Ru]**1**–[Ru]**9** are luminescent in an alcoholic rigid matrix at 77 K, with an emission lifetime value in the 3.5–5.5 μs range. The luminescence band maxima are listed in Table 6, and the luminescence spectra are given in the ESI.† In all cases, the luminescence emission clearly originates from ^{3}MLCT states involving the polypyridine ligands, as evidenced by the position and shape of the emission band, and by the lifetime values, which are in the expected range for Ru–polypyridine complexes.[31] Additional support to this assignment comes from the good

Table 4 Selected bond lengths (Å) for complexes [Ru]**1**–[Ru]**9**

Complex	[Ru]**1**	[Ru]**2**	[Ru]**3**	[Ru]**4**	[Ru]**5**	[Ru]**6**	[Ru]**7**	[Ru]**8**[a]	[Ru]**9**[a]
Ru–P	2.3104(15)	2.347(3)	2.2448(15)	2.238(2)	2.2644(16)	2.2268(11)	2.4284(19)	2.4376(9)	2.3437(16)
Ru–N1	2.103(5)	2.101(8)	2.130(5)	2.130(6)	2.113(5)	2.099(3)	2.116(6)	2.112(3)	2.090(5)

[a] From ref. 9.

Table 5 Selected NMR data of the ligands and their selenides

P(III) ligand L	**1**	**2**	**3**	**4**	**5**	**6**	**7**	**8**	**9**
δ ^{31}P L[a]/ppm	47.5	47.3	140.1	138.0	138.7	128.9	19.8	10.0	−5.7
δ ^{31}P LSe/ppm	58.4[b]	71.3[c]	72.2[b]	71.0[b]	66.6[b]	58.8[c]	69.2[c]	57.8[c]	35.4[c]
J_{PSe}/Hz	812[d]	776[e]	945[f]	940[f]	924[g]	1039[e]	716[e]	711[e]	745[e]

[a] In acetone-d_6. [b] In $CDCl_3$. [c] In toluene. [d] From ref. 28. [e] This work. [f] From ref. 29. [g] From ref. 30.

Table 6 Electrochemical and absorption data at RT in CH_3CN, and luminescence data at 77 K in EtOH : MeOH 1 : 4 (v/v). The potentials correspond to $|E_{pa} + E_{pc}|/2$ (with $E_{pa} - E_{pc}$ in parentheses)

Complex	E_{ox1}/V/SCE	E_{red1}/V/SCE	λ_{MLCT}/nm (ε/mol^{-1} L cm^{-1})	λ_{em}/nm
[Ru]**1**	+1.53 (78)	−1.16 (68)	422 (6920)	602
[Ru]**2**	+1.36[a] (73)	−1.23 (74)	440 (8140)	620
[Ru]**3**	+1.46 (74)	−1.17 (67)	417 (9590)	608
[Ru]**4**	+1.39 (74)	−1.24 (64)	421 (9020)	602
[Ru]**5**	+1.40 (93)	−1.24 (64)	423 (9640)	606
[Ru]**6**	+1.61 (98)	−1.15 (67)	401 (8400)	602
[Ru]**7**	+1.35 (83)	−1.17 (68)	461 (8650)	645
[Ru]**8**[b]	+1.32 (82)	−1.18 (64)	465 (7000)	648
[Ru]**9**[b]	+1.41 (67)	−1.22 (64)	440 (8000)	615

[a] Irreversible since $I_c/I_a = 0.5$; the oxidation potential of [Ru]**2** was also measured by square-wave (SqW) voltammetry and equals +1.38 V/SCE; for all other complexes, the potentials measured by SqW and CV differ by less than 10 mV. [b] From ref. 9.

correlation between the emission energy and the electrochemical HOMO–LUMO gap (not shown).

As opposed to the low temperature experiments, no luminescence was detected from complexes [Ru]**1**–[Ru]**9** in an acetonitrile solution at room temperature, in agreement with the general behaviour of ruthenium phosphine complexes containing bipyridine[32] or terpyridine[33] ligands. It is known that phosphine ligands have the effect of moving the emitting ^{3}MLCT state to higher energy, in close proximity to the d–d state, which plays a crucial role in determining the luminescence properties of Ru–polypyridine complexes. At room temperature the d–d state can be accessed easily by thermal activation, thus opening a non-radiative pathway for the decay of the ^{3}MLCT state. Conversely, at 77 K thermal energy is not available to reach the d–d state, and thus the ^{3}MLCT state can display the usual luminescence properties.

The common features of the UV-vis absorption spectra (see ESI†) are (i) intense ligand-centered π–π* transitions in the UV region, and (ii) a broad band in the visible region corresponding to the envelope of the Ru–bpy and Ru–tpy MLCT transitions. The wavelengths reported in Table 6 correspond to the MLCT transitions of lowest energy, *i.e.* the formal transfer of one electron from the ruthenium to the terpyridine ligand. This transition is bathochromically shifted upon increasing the overall donating power of the phosphorus ligand, ranging from 401 nm for $P(OPh)_3$ to 465 nm for PCy_3.[9] The MLCT transitions of the complexes [Ru]**1**, [Ru]**3**, [Ru]**4** and [Ru]**5** are found at around 420 nm, while those of [Ru]**2** and [Ru]**9** are red-shifted by 20 nm.

The electronic properties of complexes [Ru]**1**–[Ru]**9** were probed by electrochemistry, in an acetonitrile solution. All the cyclic voltammograms (CV) show a first reversible oxidation, except in the case of [Ru]**2**, and the first two reductions are reversible or quasi-reversible at 100 mV s^{-1} scan rate (see ESI†). For [Ru]**2**, the poor but reproducible reversibility of the oxidation process could be explained by the presence of a very minor (4% on the basis of current intensities) irreversible couple at E_{pa}= 0.62 V/SCE and E_{pc}= 0.49 V/SCE, corresponding to a species, which was not detected by ^{1}H NMR, and could not be identified by comparison with known redox couples. The extra wave seen in the reduction of [Ru]**2** at E_{pa} = –0.24 V/SCE, is also reproducible and corresponds to the back oxidation of the component that is irreversibly reduced at E_{pc} = −1.70 V/SCE (see ESI†). The elucidation of this latter phenomenon is out of the scope of this work and does not interfere with the processes under discussion (*i.e.* first oxidation and first reduction).

In comparison with the literature, and on the basis of DFT calculations performed on $[Ru(tpy)(bpy)(DMSO)]^{2+}$,[34] $[Ru(bpy)_3]^{2+}$,[35] and $[Ru(tpy)_2]^{2+}$,[36] the oxidation is assigned to a metal-centered process and the first two reductions involve mostly the polypyridine ligands. The first reduction, centered on the most delocalized terpyridine ligand, is relevant for comparison purposes with the MLCT transition of lowest energy. Indeed, the transition corresponding to the formal transfer of one electron from the metal to the most reducible ligand (*i.e.* optical gap) should correlate with the Ru^{III}/Ru^{II} and $tpy/tpy^{-\bullet}$ redox potentials (*i.e.* electrochemical gap) (Fig. 4).[37]

Regarding the ruthenium oxidation potential in the $[Ru(tpy)(bpy)L]^{2+}$ complexes, it appears in the order $PCy_3 \approx P^iPr_3 \approx Ph_2P$-pyrrolidinyl < $P(OEt)_3 \approx P(O^iPr)_3 \approx PPh_3 < P(OMe)_3 < Ph_2P$-pyrrolyl < $P(OPh)_3$. Indeed an electron-rich ligand such as PCy_3 or P^iPr_3 should efficiently stabilize the Ru^{III} state and hence, should lower the oxidation potential. The differences between the relative order of the J_{PSe} values and the relative order of the E_{ox} values is due to the fact that the coupling constant of the selenide derivative only gives an estimate of the basicity, or σ-donating capacity, of the phosphorus atom, whereas the redox potentials are under the influence of a combination of donating and accepting σ and π effects.[24]

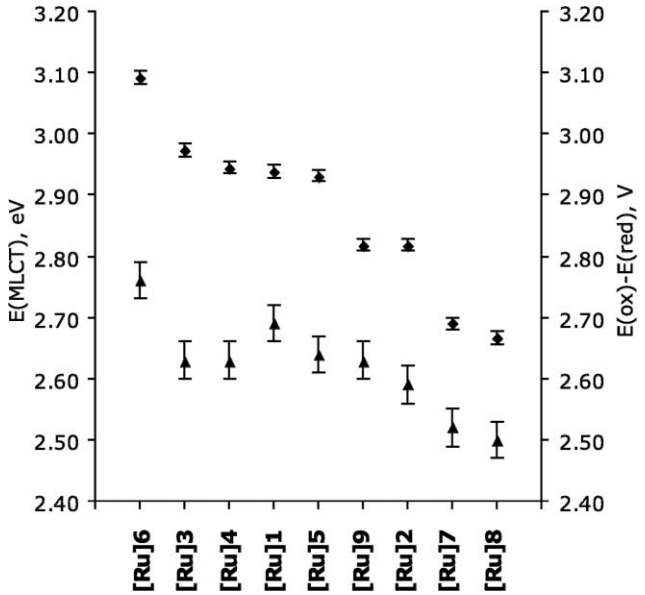

Fig. 4 Correlation between optical (diamonds) and electrochemical (triangles) gaps. The error bars are given for the uncertainties of ±2 nm on λ_{MLCT} and ±15 mV for redox potentials.

The most striking feature of this electrochemical study lies in the fact that the simple variation of the substituents on a neutral phosphorus(III) ligand allows to cover a potential range of 290 mV, a range, which is not accessible for ruthenium polypyridine complexes bearing a sixth neutral nitrogen ligand (Chart 1).[38] In addition, it is noteworthy that phosphorus(III) ligands strongly stabilize the Ru^{II} oxidation state as compared to nitrogen ligands.

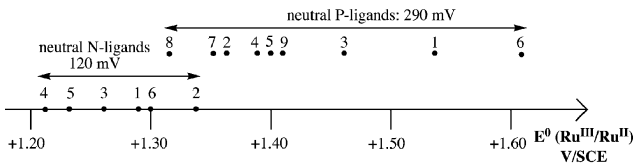

Neutral nitrogen ligands :
acetonitrile (1)
benzonitrile (2)
pyridine (3)
4-vinylpyridine (4)
4-cyanopyridine (5)
pyrazine (6)

Neutral phosphorus ligands :
diphenylpyrrolylphosphine (1)
diphenylpyrrolidinylphosphine (2)
trimethylphosphite (3)
triethylphosphite (4)
triisopropylphosphite (5)
triphenylphosphite (6)
triisopropylphosphine (7)
tricyclohexylphosphine (8)
triphenylphosphine (9)

Chart 1 Accessible Ru^{III}/Ru^{II} potential range with neutral nitrogen and phosphorus ligands in $[Ru(tpy)(bpy)L]^{2+}$ complexes

The first reduction is expected to be predominantly terpyridine-centered and varies over a narrow potential range of 90 mV (Table 6). We found essentially two different values for this reduction: –1.17 V/SCE for Ph_2P-pyrrolyl, $P(OMe)_3$, $P(OPh)_3$, P^iPr_3 and PCy_3, and –1.23 V/SCE for Ph_2P-pyrrolidinyl, $P(OEt)_3$, $P(O^iPr)_3$ and PPh_3. Although the reduced state should intuitively be stabilized by the most π-accepting ligands, this trend is not found experimentally throughout the whole series. As discussed by Giering *et al.* in their QALE approach,[39] meaningful comparisons can be made within a family of ligands but not always between families, or 'classes'. The trend in the phosphine family is unexpected but the difference is small between $E_{red}(PR_3)$ and $E_{red}(PAr_3)$, and given the inherent experimental uncertainty of cyclic voltammetry, a discussion around small potential variations should be done with extreme caution. Within the aminophosphine and phosphite families, the expected trend is found experimentally and underlines the importance of the impact of the heteroatom (N, O) coordinated α to the phosphorus upon its electron-donating and accepting properties.

Conclusions

This is the first report of the coordination of aminophosphines and phosphites onto a ruthenium bipyridine terpyridine complex. For all the complexes described in this study, the X-ray diffraction structures show a classical monodentate coordination on the phosphorus atom. The electronic properties of the complexes were probed by the means of electrochemistry, absorption spectroscopy and luminescence studies. It appears that the range of properties allowed by a single neutral two-electron phosphorus(III) ligand is very broad, the MLCT transition wavelength spanning over 65 nm and the Ru^{III}/Ru^{II} redox potential ranging over 290 mV between the two extremes of this study, $[Ru(tpy)(bpy)P(OPh)_3]^{2+}$ and $[Ru(tpy)(bpy)PCy_3]^{2+}$. It is remarkable that such a broad range is unprecedented for neutral L-type ligands coordinated by the same heteroatom, in this case phosphorus(III). Further work is underway to synthesize phosphorus ligands with more elaborate heteroatomic substituents in order to fine-tune the electronic properties of the corresponding ruthenium polypyridine complexes.

Experimental

Ligands **3–7** are commercially available and were used without further purification. $Ru(tpy)(bpy)(NCCH_3)(PF_6)_2$ was synthesized from $[Ru(tpy)(bpy)Cl](PF_6)$ according to the method described for $Ru(tpy)(phen)(NCCH_3)(PF_6)_2$.[13] The abbreviations tpy and bpy stand for 2,2′:6′,2″-terpyridine and 2,2′-bipyridine respectively, and [Ru] stands for $Ru(tpy)(bpy)(PF_6)_2$. All solvents were dried and distilled by standard methods. Column chromatography was performed on silica gel from SDS (70–200 μm), using the ternary mixture acetone–H_2O–saturated aqueous KNO_3 solution 90 : 5 : 0.5 as starting eluent, followed by a gradual increase of the H_2O–KNO_3 amount. NMR spectra were performed on a Bruker AV300 spectrometer, in $(CD_3)_2CO$ unless otherwise stated.

Monocrystals of all the complexes were obtained by the slow liquid diffusion of diethylether into an acetone solution of the complex. For X-ray analysis, data were collected at low temperature on an Oxford Diffraction Xcalibur for **1**·BH_3, **2**·Se, [Ru]**1**, [Ru]**4**, [Ru]**5**, [Ru]**6** and [Ru]**7**, and on a Oxford Diffraction Gemini for [Ru]**3**, using graphite monochromated Mo Kα radiation (λ = 0.71073 Å), and equipped with an Oxford Instrument Cooler Device. For [Ru]**2**, data were collected on a STOE-IPDS equipped with an Oxford Cryosystems Cryostream Cooler Device, using graphite monochromated Mo Kα radiation (λ = 0.71073 Å). The final unit cell parameters have been obtained by means of a least-squares refinement. The structures have been solved by direct methods using SIR92,[40] and refined by means of least-squares procedures on F^2 with the program SHELXL-97,[41] included in the software package WinGX version 1.63,[42] except for the structure [Ru]**2**, which was refined on F using Crystal.[43] The atomic scattering factors were taken from the

international tables for X-ray crystallography.[44] All hydrogens atoms were geometrically placed and refined by using a riding model. All non-hydrogens atoms were anisotropically refined, and in the last cycles of refinement a weighting scheme was used, where weights are calculated from the following formula: $w = 1/[\sigma^2(F_o^2) + (aP)^2 + bP]$ where $P = (F_o^2 + 2F_c^2)/3$. The disorder models for [Ru]**1**, [Ru]**4**, [Ru]**5**, and [Ru]**7** are the following: for [Ru]**1** the disorders on two aromatic cycles were treated using the PART command in SHELXL-97. One PF_6 is highly disordered, such a disorder is not treated easily with the PART command in SHELXL-97, since the F atoms are not disordered over only two sites. This results in several ALERT-B in the checkcif. Concerning [Ru]**4**, [Ru]**5** and [Ru]**7**, the disorders of the carbon atoms of the phosphorus moiety were treated using the PART command in SHELXL-97. For complexes [Ru]**4** and [Ru]**7**, it was not possible to properly resolve the diffuse electron density residuals related to an acetone crystallization solvent molecule. Treatment with the SQUEEZE facility from PLATON[45] with a localized void of about 2106.3 Å^3 and 378 recovered electrons for [Ru]**4** and with a localized void of about 624.3 Å^3 and 109 recovered electrons for [Ru]**7** resulted in a smooth refinement. Since a few low-order reflections are missing from the data set, the electron count is underestimated. Consequently, the values given for ρ_{calcd}, $F(000)$ and the formula weight are only valid for the ordered part of the structures. Figures of the molecules were drawn with the program ORTEP3,[46] with 30% probability displacement ellipsoids for non-hydrogen atoms.

The electrochemical measurements were obtained using an Autolab PGSTAT 100 potentiostat using tetrabutylammonium hexafluorophosphate as the supporting electrolyte in freshly distilled acetonitrile and a platinum working electrode. Electrospray mass spectrometry analyses were performed on a Perkin Elmer Sciex API-365 spectrometer in positive mode. Melting points were determined in capillaries using an Electrothermal melting point apparatus. Luminescence experiments were conducted in air-equilibrated acetonitrile solutions at room temperature, and in an EtOH–MeOH 1 : 4 v/v matrix at 77 K. Uncorrected emission spectra and emission lifetimes were obtained with an Edinburgh FLS-920 spectrofluorimeter. Emission spectra at 77 K were recorded using quartz tubes immersed in a quartz Dewar filled with liquid nitrogen. Scheme 1 shows the numbering used for the ligands and complexes.

Complex [Ru]1

Ligand **1** (250 mg, 1 mmol) and the complex [Ru]$NCCH_3$ (85 mg, 0.1 mmol) were placed in a closed Schlenk tube with freshly distilled acetone (4 mL) and irradiated for 2 h. After cooling, the reaction mixture was poured into an excess of diethylether to precipitate the complexes. The precipitate was recovered by filtration, washed with diethylether, taken in acetone and chromatographed on silica gel (acetone–H_2O–saturated aqueous KNO_3 (v/v) from 100 : 5 : 0.5–100 : 8 : 0.8). In a final step, the nitrate counter ions were replaced by hexafluorophosphate ions to ensure solubility in organic solvents. Complex [Ru]**1** was isolated in 47% yield (50 mg) as a bright orange solid. δ_H (ppm) = 9.39 (d, 1H, H_a, ^3J = 6.0 Hz), 8.98 (d, 1H, H_d, ^3J = 8.1 Hz), 8.80 (d, 1H, H_g, ^3J = 8.1 Hz), 8.54 (d, 2H, $H_{3'}$, ^3J = 8.1 Hz), 8.50–8.43 (m, 3H, H_3 + H_c), 8.32 (t, 1H, $H_{4'}$, ^3J = 8.1 Hz), 8.29 (d, 2H, H_6, ^3J = 5.4 Hz), 8.15–8.08 (m, 4H, H_h + H_4 + H_i), 7.85 (dd, 1H, H_b, $^3J = {}^3J$ = 6.4 Hz), 7.55–7.46 (m, 4H, H_5 + H_p), 7.37 (m, 1H, H_j), 7.34–7.24 (m, 4H, H_o), 6.84–6.74 (m, 6H, H_m + NC*H*CH), 6.33 (s, 2H, NCHC*H*). δ_P (ppm) = 92.2, −144.2 (sept, J_{PF} = 708 Hz). δ_C (ppm) = 157.81 (C_2), 157.28 (d, C_e, J = 2.2 Hz), 156.70 ($C_{2'}$), 156.61 (d, C_a, J = 3.8 Hz), 155.71 (C_f), 154.43 (C_6), 148.55 (d, C_j, J = 1.4 Hz), 139.67 (C_h), 139.29 (C_4), 139.08 (C_c), 137.81 ($C_{4'}$), 131.47 (d, C_p, J = 2.2 Hz), 130.64 (d, C_m, J = 10.9 Hz), 129.08 (d, C_{ipso}, J = 46.5 Hz), 129.27 (d, C_o, J = 9.8 Hz), 128.62 (C_5), 127.94 (C_b), 127.82 (d, C_i, J = 2.1 Hz), 126.02 (d, N*C*HCH, J = 4.4 Hz), 125.37 (C_d), 124.86 (C_3), 124.70 ($C_{3'}$), 124.24 (d, C_g, J = 2.1 Hz), 113.00 (d, NCH*C*H, J= 5.3 Hz). ES$^+$-MS: m/z = 886.9 ([M–PF_6]$^+$), 371.1 ([M–2PF_6]$^{2+}$), mp 260 °C (decomposition).

Complex [Ru]2

Ligand **2** (250 mg, 1 mmol) and the complex [Ru]$NCCH_3$ (82 mg, 0.1 mmol) were placed in a closed Schlenk tube with freshly distilled acetone (4 mL) and were irradiated for 2 h. After cooling, the reaction mixture was poured into an excess of diethylether to precipitate the complexes. The precipitate was recovered by filtration, washed with diethylether, taken in acetone and chromatographed on silica gel (acetone–H_2O–saturated aqueous KNO_3 (v/v) from 100 : 5 : 0.5–100 : 6 : 0.6). In a final step, the nitrate counter ions were replaced by hexafluorophosphate ions to ensure solubility in organic solvents. Complex [Ru]**2** was isolated in 92% yield (95 mg) as a bright orange solid. δ_H (ppm) = 10.23 (d, 1H, H_a, ^3J = 6.0 Hz), 8.96 (d, 1H, H_d, ^3J = 6.0 Hz), 8.75 (d, 1H, H_g, ^3J = 9.0 Hz), 8.50 (ddd, 1H, H_c, $^3J = {}^3J$ = 8.0 Hz, ^4J = 1.3 Hz), 8.43 (d, 2H, $H_{3'}$, ^3J = 8.1 Hz), 8.42 (d, 2H, H_3, ^3J = 7.8 Hz), 8.25–8.15 (m, 2H, H_b + $H_{4'}$), 8.10 (d, 2H, H_6, ^3J = 5.7 Hz), 8.08–8.00 (m, 3H, H_h + H_4), 7.42–7.35 (m, 4H, H_p + H_5), 7.30–7.20 (m, 6H, H_m + H_i + H_j), 7.04 (t, 4H, H_o, ^3J = 8.7 Hz), 3.02 (m, 4H, NCH_2CH_2), 1.86 (m, 4H, NCH_2CH_2). δ_P (ppm) = 78.1, −144.2 (sept, $^1J_{PF}$ = 705 Hz). δ_C (ppm) = 157.83 (C_2), 157.15 (d, C_e, J = 2.3 Hz), 156.71 ($C_{2'}$), 156.61 (d, C_a, J = 3.0 Hz), 155.72 (C_f), 154.38 (C_6), 148.46 (d, C_j, J = 0.8 Hz), 139.14 (C_h), 138.60 (C_4 + C_c), 136.76 ($C_{4'}$), 130.91 (d, C_o, J = 9.8 Hz), 130.11 (d, C_p, J = 2.3 Hz), 129.87 (d, C_{ipso}, J= 46.8 Hz), 128.74 (d, C_m, J= 9.0 Hz), 128.28 (C_b), 128.11 (C_5), 127.56 (d, C_i, J = 2.3 Hz), 125.12 (C_d), 124.31 (C_3), 124.10 ($C_{3'}$), 124.00 (d, C_g, J = 1.5 Hz), 50.68 (N*C*H_2CH_2), 26.06 (d, NCH_2*C*H_2, J = 6.6 Hz). ES$^+$-MS: m/z = 891.3 ([M–PF_6]$^+$), 373.0 ([M–2PF_6]$^{2+}$), mp 197 °C.

Complex [Ru]3

Trimethylphosphite (150 μL, 1.2 mmol) and the complex [Ru]-$NCCH_3$ (100 mg, 0.12 mmol) were placed in a closed Schlenk tube with freshly distilled acetone (4 mL) and were irradiated for 2 h. After cooling, the reaction mixture was poured into an excess of diethylether to precipitate the complexes. The precipitate was recovered by filtration, washed with diethylether, taken in acetone and chromatographed on silica gel (acetone–H_2O–saturated aqueous KNO_3 (v/v) from 90 : 5 : 0.5–90 : 6 : 0.6). In a final step, the nitrate counter ions were replaced by hexafluorophosphate ions to ensure solubility in organic solvents. Complex [Ru]**3** was isolated in 79% yield (88 mg) as a bright orange solid. δ_H (ppm) = 9.92 (d, 1H, H_a, ^3J = 5.4 Hz), 8.91 (d, 1H, H_d, ^3J = 8.4 Hz), 8.87 (d, 2H, $H_{3'}$, ^3J = 8.1 Hz), 8.78–8.68 (m, 3H, H_g + H_3),

8.55 (t, 1H, $H_{4'}$, $^3J = 8.1$ Hz), 8.44 (dd, 1H, H_c, $^3J = {}^3J = 7.7$ Hz), 8.20 (dd, 2H, H_4, $^3J = {}^3J = 7.5$ Hz), 8.16–8.02 (m, 4H, $H_b + H_h + H_6$), 7.60–7.50 (m, 3H, $H_j + H_5$), 7.39 (dd, 1H, H_i, $^3J = {}^3J = 6.5$ Hz), 3.46 (d, 9H, $P(OCH_3)_3$, $^3J_{HP} = 10.5$ Hz). δ_P (ppm) = 126.3 (decaplet, $^3J_{HP} = 10$ Hz), −144.3 (sept, $^1J_{PF} = 708$ Hz). δ_C (ppm) = 157.91 (C_2), 157.20 ($C_{2'}$), 156.69 (d, C_e, $J = 2.9$ Hz), 155.90 (d, C_a, $J = 2.5$ Hz), 155.36 (d, C_f, $J = 1.4$ Hz), 153.70 (C_6), 148.21 (d, C_j, $J = 1.5$ Hz), 139.39 (C_h), 139.11 (C_4), 138.43 (C_c), 138.09 ($C_{4'}$), 128.33 (C_5), 128.16 (d, C_b, $J = 0.7$ Hz), 127.49 (d, C_i, $J = 3.5$ Hz), 124.84 (C_d), 124.66 (C_3), 123.98 ($C_{3'}$), 123.77 (d, C_g, $J = 2.9$ Hz), 53.00 (d, $P(OCH_3)_3$, $J = 8.6$ Hz). ES$^+$-MS: $m/z = 750.56$ ($[M–PF_6]^+$), 307.98 ($[M–2PF_6]^{2+}$), mp 244 °C (decomposition).

Complex [Ru]4

Triethylphosphite (140 μL, 0.8 mmol) and the complex [Ru]$NCCH_3$ (67 mg, 0.08 mmol) were placed in a closed Schlenk tube with freshly distilled acetone (4 mL) and were irradiated for 2 h. After cooling, the reaction mixture was poured into an excess of diethylether to precipitate the complexes. The precipitate was recovered by filtration, washed with diethylether, taken in acetone and chromatographed on silica gel (acetone–H_2O–saturated aqueous KNO_3 (v/v) from 100 : 5 : 0.5–100 : 7 : 0.7). In a final step, the nitrate counter ions were replaced by hexafluorophosphate ions to ensure solubility in organic solvents. Complex [Ru]**4** was isolated in 86% yield (66 mg) as a bright orange solid. δ_H (ppm) = 9.95 (d, 1H, H_a, $^3J = 5.7$ Hz), 8.93–8.83 (m, 3H, $H_d + H_{3'}$), 8.77–8.68 (m, 3H, $H_g + H_3$), 8.54 (t, 1H, $H_{4'}$, $^3J = 8.1$ Hz), 8.44 (dd, 1H, H_c, $^3J = {}^3J = 7.8$ Hz), 8.20 (dd, 2H, H_4, $^3J = {}^3J = 7.8$ Hz), 8.15–8.02 (m, 4H, $H_b + H_h + H_6$), 7.61–7.51 (m, 3H, $H_j + H_5$), 7.40 (dd, 1H, H_i, $^3J = {}^3J = 6.6$ Hz), 3.82 (m, 6H, $POCH_2CH_3$), 0.97 (t, 9H, $POCH_2CH_3$, $^3J = 6.9$ Hz). δ_P (ppm) = 121.6, −144.2 (sept, $^1J_{PF} = 708$ Hz). δ_C (ppm) = 158.00 (C_2), 157.23 ($C_{2'}$), 156.76 (large, C_e), 155.68 (d, C_a, $J = 2.7$ Hz), 155.34 (d, C_f, $J = 1.5$ Hz), 153.62 (C_6), 148.44 (d, C_j, $J = 1.2$ Hz), 139.31 (C_h), 138.98 (C_4), 138.40 (C_c), 137.84 ($C_{4'}$), 128.28 (C_5), 128.01 (C_b), 127.45 (d, C_i, $J = 3.5$ Hz), 124.84 (C_d), 124.53 (C_3), 123.90 ($C_{3'}$), 123.75 (d, C_g, $J = 2.8$ Hz), 62.39 (d, $POCH_2CH_3$, $J =$ 8.9 Hz), 15.40 ($POCH_2CH_3$). ES$^+$-MS: $m/z = 802.2$ ($[M–PF_6]^+$), 328.5 ($[M–2PF_6]^{2+}$), mp 255 °C.

Complex [Ru]5

Tri(isopropyl)phosphite (275 μL, 1.2 mmol) and the complex [Ru]$NCCH_3$ (99 mg, 0.12 mmol) were placed in a closed Schlenk tube with freshly distilled acetone (4 mL) and were irradiated for 2 h. After cooling, the reaction mixture was poured into an excess of diethylether to precipitate the complexes. The precipitate was recovered by filtration, washed with diethylether, taken in acetone and chromatographed on silica gel (acetone–H_2O–saturated aqueous KNO_3 (v/v) from 90 : 5 : 0.5–90 : 7 : 0.7). In a final step, the nitrate counter ions were replaced by hexafluorophosphate ions to ensure solubility in organic solvents. Complex [Ru]**5** was isolated in 91% yield (109 mg) as a bright orange solid. δ_H (ppm) = 9.91 (d, 1H, H_a, $^3J = 5.4$ Hz), 8.96–8.88 (m, 3H, $H_d + H_{3'}$), 8.77–8.70 (m, 3H, $H_g + H_3$), 8.55 (t, 1H, $H_{4'}$, $^3J = 8.4$ Hz), 8.46 (dd, 1H, H_c, $^3J = {}^3J = 7.8$ Hz), 8.24–8.07 (m, 6H, $H_4 + H_b + H_h + H_6$), 7.60–7.52 (m, 3H, $H_5 + H_j$), 7.38 (dd, 1H, H_i, $^3J = {}^3J = 6.5$ Hz), 4.62–4.44 (m, 3H, $CHCH_3$), 0.98 (d, 18H, $^3J = 6.0$ Hz, $CHCH_3$). δ_P (ppm) = 118.3 (d, $J = 5.8$ Hz), −144.2 (sept, $^1J_{PF} = 708$ Hz). δ_C (ppm) = 158.10 (C_2), 157.30 ($C_{2'}$), 156.82 (d, C_e, $J = 2.8$ Hz), 155.74 (d, C_a, $J = 2.9$ Hz), 155.33 (d, C_f, $J = 1.6$ Hz), 153.84 (C_6), 148.62 (d, C_j, $J = 1.4$ Hz), 139.30 (C_h), 138.92 (C_4), 138.50 (C_c), 137.72 ($C_{4'}$), 128.42 (C_5), 127.75 (C_b), 127.47 (d, C_i, $J = 3.5$ Hz), 124.96 (C_d), 124.41 (C_3), 123.93 ($C_{3'}$), 123.81 (d, C_g, $J = 2.9$ Hz), 71.45 (d, $CHCH_3$, $J = 9.5$ Hz), 23.24 (d, $CHCH_3$, $J = 3.7$ Hz). ES$^+$-MS: $m/z = 844.20$ ($[M–PF_6]^+$), 349.74 ($[M–2PF_6]^{2+}$), mp 242 °C.

Complex [Ru]6

Triphenylphosphite (265 μL, 1 mmol) and the complex [Ru]$NCCH_3$ (83 mg, 0.1 mmol) were placed in a closed Schlenk tube with freshly distilled acetone (4 mL) and were irradiated for 2 h. After cooling, the reaction mixture was poured into an excess of diethylether to precipitate the complexes. The precipitate was recovered by filtration, washed with diethylether, taken in acetone and chromatographed on silica gel (acetone–H_2O–saturated aqueous KNO_3 (v/v) from 100 : 5 : 0.5–100 : 8 : 0.8). In a final step, the nitrate counter ions were replaced by hexafluorophosphate ions to ensure solubility in organic solvents. Complex [Ru]**6** was isolated in 91% yield (100 mg) as a pale orange solid. δ_H (ppm) = 10.38 (d, 1H, H_a, $^3J = 5.7$ Hz), 8.93 (d, 1H, H_d, $^3J = 8.1$ Hz), 8.72 (d, 1H, H_g, $^3J = 8.1$ Hz), 8.64 (d, 2H, $H_{3'}$, $^3J =$ 8.1 Hz), 8.59 (d, 2H, H_3, $^3J = 8.1$ Hz), 8.53 (dd, 1H, H_c, $^3J = {}^3J =$ 8.1 Hz), 8.42 (t, 1H, $H_{4'}$, $^3J = 8.1$ Hz), 8.32 (dd, 1H, H_b, $^3J = {}^3J =$ 6.6 Hz), 8.15–8.05 (m, 3H, $H_h + H_4$), 7.89 (d, 2H, H_6, $^3J = 5.4$ Hz), 7.38 (dd, 1H, H_i, $^3J = {}^3J = 6.6$ Hz), 7.30 (dd, 2H, H_5, $^3J = {}^3J =$ 6.6 Hz), 7.25 (dd, 1H, H_j, $^3J = {}^3J = 4.7$ Hz), 7.19–7.05 (m, 9H, $H_m + H_p$), 6.84 (d, 6H, H_o, $^3J = 8.1$ Hz). δ_P (ppm) = 115.4, −144.2 (sept, $J_{PF} = 708$ Hz). δ_C (ppm) = 157.55 (C_2), 156.83 (d, C_e, $J =$ 2.9 Hz), 156.73 ($C_{2'}$), 155.80 (d, C_a, $J = 2.6$ Hz), 155.29 (d, C_f, $J = 1.4$ Hz), 153.62 (C_6), 151.01 (d, C_{ipso}, $J = 11.2$ Hz), 147.41 (d, C_j, $J = 1.2$ Hz), 139.93 (C_h), 139.41 (C_4), 139.29 ($C_{4'}$), 139.19 (C_c), 130.34 (C_m), 128.72 (C_5), 128.63 (C_b), 127.87 (d, C_i, $J = 3.5$ Hz), 125.33 (C_p), 125.27 (C_d), 125.18 (C_3), 124.46 ($C_{3'}$), 124.05 (d, C_g, $J = 2.9$ Hz), 119.37 (d, C_o, $J = 4.7$ Hz). ES$^+$-MS: $m/z = 945.9$ ($[M–PF_6]^+$), 400.5 ($[M–2PF_6]^{2+}$), mp 248 °C (decomposition).

Complex [Ru]7

Tri(isopropyl)phosphine (190 μL, 1 mmol) and the complex [Ru]$NCCH_3$ (82 mg, 0.1 mmol) were placed in a closed Schlenk tube with freshly distilled acetone (4 mL) and were irradiated for 2 h. After cooling, the reaction mixture was poured into an excess of diethylether to precipitate the complexes. The precipitate was recovered by filtration, washed with diethylether, taken in acetone and chromatographed on silica gel (acetone–H_2O–saturated aqueous KNO_3 (v/v) from 90 : 5 : 0.5–90 : 10 : 1). In a final step, the nitrate counter ions were replaced by hexafluorophosphate ions to ensure solubility in organic solvents. Complex [Ru]**7** was isolated in 63% yield (60 mg) as a bright orange solid. δ_H (ppm) = 9.87 (d, 1H, H_a, $^3J = 5.7$ Hz), 9.00–8.87 (m, 3H, $H_d + H_{3'}$), 8.72 (d, 2H, H_3, $^3J = 7.8$ Hz), 8.66 (d, 1H, H_g, $^3J = 7.8$ Hz), 8.55–8.42 (m, 2H, $H_c + H_{4'}$), 8.24 (d, 2H, H_6, $^3J = 5.4$ Hz), 8.20–8.10 (m, 3H, $H_4 + H_b$), 7.98 (dd, 1H, H_h, $^3J = {}^3J = 7.8$ Hz), 7.52 (dd, 2H, H_5, $^3J =$ $^3J = 6.4$ Hz), 7.26 (dd, 1H, H_i, $^3J = {}^3J = 6.6$ Hz), 6.98 (d, 1H, H_j, $^3J = 5.4$ Hz), 2.25 (m, 3H, $CHCH_3$), 0.91 (m, 18H, $CHCH_3$). δ_P

(ppm) = 29.4 (broad), −144.2 (sept, J_{PF} = 708 Hz). δ_C (ppm) = 158.82 ($C_{2'}$), 158.73 (C_2), 156.98 (d, C_a, J = 1.6 Hz), 156.90 (d, C_e, J = 2.1 Hz), 156.14 (C_f), 154.71 (C_6), 147.09 (C_j), 138.96 (C_4), 138.81 (C_h), 138.75 (C_c), 137.39 ($C_{4'}$), 128.25 (C_5), 128.00 (C_b), 127.63 (d, C_i, J = 1.7 Hz), 125.09 (C_d), 124.80 (C_3), 124.53 ($C_{3'}$), 123.86 (d, C_g, J = 1.6 Hz), 24.44 (d, $CHCH_3$, J = 19.4 Hz), 18.75 ($CHCH_3$). ES^+-MS: m/z = 796.0 ($[M–PF_6]^+$), 325.6 ($[M–2PF_6]^{2+}$), mp 229 °C (decomposition).

Acknowledgements

We thank the French Ministry of Education for a Ph.D. fellowship to EL and Dr A. Sournia-Saquet for the electrochemical measurements. Johnson Matthey is gratefully acknowledged for a loan of $RuCl_3 \cdot xH_2O$. We would like to thank Oxford Diffraction, especially Dr Neil Brooks, for technical assistance and for recording the diffracted intensities of complex [Ru]**3** on their demonstration Gemini R diffractometer. This work has been supported in Italy by MIUR grant FIRB (LaTEMAR: Laboratorio di Tecnologie Elettrobiochimiche Miniaturizzate per l'Analisi e la Ricerca).

References

1 N. Armaroli and V. Balzani, V., *Angew. Chem., Int. Ed.*, 2007, **46**, 52.
2 A. Shalav, *Prog. Photovoltaics*, 2006, **14**, 675.
3 M. K. Nazeeruddin, ed., *Coord. Chem. Rev.*, 2004, **248**, 1161.
4 B. O'Regan and M. Grätzel, *Nature*, 1991, **353**, 737.
5 M. K. Nazeeruddin and M. Grätzel, *Compr. Coord. Chem. II.*, 2004, **9**, 719; M. K. Nazeeruddin and M. Grätzel, *Struct. Bonding*, 2007, **123**, 113.
6 B. Li, L. Wang, B. Kang, P. Wang and Y. Qiu, *Sol. Energy Mater. Sol. Cells*, 2006, **90**, 549, and references therein.
7 W. U. Huynh, J. J. Dittmer and A. P. Alivisatos, *Science*, 2002, **295**, 2425; M. Adachi, Y. Murata, I. Okada and S. Yoshikawa, *J. Electrochem. Soc.*, 2003, **150**, G488; J.-H. Yoon, S.-R. Jang, R. Vittal, J. Lee and K.-J. Kim, *J. Photochem. Photobiol., A*, 2006, **180**, 184; B. Tan, E. Toman, Y. Li and Y. Wu, *J. Am. Chem. Soc.*, 2007, **129**, 4162.
8 N. Robertson, *Angew. Chem., Int. Ed.*, 2006, **45**, 2338; N. Robertson, *Angew. Chem., Int. Ed.*, 2008, **47**, 1012.
9 E. Lebon, I. M. Dixon, L. Vendier, A. Igau and P. Sutra, *Inorg. Chim. Acta*, 2007, **360**, 1235.
10 N. C. Fletcher and F. R. Keene, *J. Chem. Soc., Dalton Trans.*, 1998, 2293.
11 O. Kühl, *Coord. Chem. Rev.*, 2005, **249**, 693, and references therein.
12 C. A. Tolman, *Chem. Rev.*, 1977, **77**, 313.
13 K. G. Moloy and J. L. Petersen, *J. Am. Chem. Soc.*, 1995, **117**, 7696.
14 A. Fernandez, C. Reyes, T. Y. Lee, A. Prock, W. P. Giering, C. M. Haar and S. P. Nolan, *J. Chem. Soc., Perkin Trans. 2*, 2000, 1349.
15 A. Suarez, M. A. Mendez-Rojas and A. Pizzano, *Organometallics*, 2002, **21**, 4611.
16 S. M. Socol and J. G. Verkade, *Inorg. Chem.*, 1984, **23**, 3487; T. S. Barnard and M. R. Mason, *Organometallics*, 2001, **20**, 206.
17 P. W. Dyer, J. Fawcett, M. J. Hanton, R. D. W. Kemmitt, R. Padda and N. Singh, *Dalton Trans.*, 2003, 104.
18 J.-M. Brunel, B. Faure and M. Maffei, *Coord. Chem. Rev.*, 1998, **178–180**, 665; B. Carboni and L. Monnier, *Tetrahedron*, 1999, **55**, 1197.
19 H. Noth and E. Z. Fluck, *Z. Naturforsch., B: Anorg. Chem., Org. Chem.*, 1984, **39**, 744; S. Jugé, M. Stephan, R. Merdès, J.-P. Genet and S. Halut-Desportes, *J. Chem. Soc., Chem. Commun.*, 1993, 531; A. J. Rippert, A. Linden and H.-J. Hansen, *Helv. Chim. Acta*, 2000, **83**, 311; C. Bauduin, D. Moulin, E. B. Kaloun, C. Darcel and S. Jugé, *J. Org. Chem.*, 2003, **68**, 4293.
20 K. Maartmann-Moe, C. Roemming and J. Songstad, *Acta Chem. Scand., Ser. A*, 1982, **36**, 757; M. R. I. Zubiri, H. L. Milton, D. J. Cole-Hamilton, A. M. Z. Slawin and J. D. Woollins, *Polyhedron*, 2004, **23**, 693; M. S. Balakrishna, P. P. George and J. T. Mague, *Phosphorus, Sulfur Silicon Relat. Elem.*, 2006, **181**, 141.
21 S. Bonnet, J.-P. Collin, N. Gruber, J.-P. Sauvage and E. R. Schofield, *Dalton Trans.*, 2003, 4654.
22 C. R. Hecker, P. E. Fanwick and D. R. McMillin, *Inorg. Chem.*, 1991, **30**, 659.
23 E. Sondaz, A. Gourdon, J.-P. Launay and J. Bonvoisin, *Inorg. Chim. Acta*, 2001, **316**, 79.
24 L. Perrin, E. Clot, O. Eisenstein, J. Loch and R. H. Crabtree, *Inorg. Chem.*, 2001, **40**, 5806.
25 C. Janiak, *J. Chem. Soc., Dalton Trans.*, 2000, 3885.
26 D. W. Allen and B. F. Taylor, *J. Chem. Soc., Dalton Trans.*, 1982, 51.
27 N. G. Andersen and B. A. Keay, *Chem. Rev.*, 2001, **101**, 997.
28 C. E. Anderson, A. S. Batsanov, P. W. Dyer, J. Fawcett and J. A. K. Howard, *Dalton Trans.*, 2006, 5362.
29 E. Krawczyk, A. Skowronska and J. Michalski, *J. Chem. Soc., Perkin Trans. 2*, 2000, 1135.
30 C. Glidewell and E. J. Leslie, *J. Chem. Soc., Dalton Trans.*, 1977, 527.
31 A. Juris, V. Balzani, F. Barigelletti, S. Campagna, P. Belser and A. von Zelewsky, *Coord. Chem. Rev.*, 1988, **84**, 85; K. Kalyanasundaram, *Photochemistry of Polypyridine and Porphyrin Complexes*, Academic Press, London, 1992.
32 J. V. Caspar and T. J. Meyer, *Inorg. Chem.*, 1983, **22**, 2444; M. L. Myrick and M. K. De Armond, *J. Phys. Chem.*, 1989, **93**, 7099; V. Wing-Wah Yam, V. Wing-Man Lee and K.-K. Cheung, *J. Chem. Soc., Dalton Trans.*, 1997, 2335; B. Hong, S. R. Woodcock, S. K. Saito and J. V. Ortega, *J. Chem. Soc., Dalton Trans.*, 1998, 2615; S. V. Litke, T. V. Mezentseva, A. S. Litke, G. N. Lyalin and A. Yu. Ershov, *Opt. Spektrosk.*, 2000, **89**, 847; T. Suzuki, T. Kuchiyama, S. Kishi, S. Kaizaki, H. D. Takagi and M. Kato, *Inorg. Chem.*, 2003, **42**, 785; J. M. Butler, G. M. Gray and J. P. Claude, *Polyhedron*, 2004, **23**, 1719.
33 B. J. Coe, D. W. Thompson, C. T. Culbertson, J. R. Schoonover and T. J. Meyer, *Inorg. Chem.*, 1995, **34**, 3385; M. Gagliardo, H. P. Dijkstra, P. Coppo, L. De Cola, M. Lutz, A. L. Spek, G. P. M. van Klink and G. van Koten, *Organometallics*, 2004, **23**, 5833.
34 I. Ciofini, C. A. Daul and C. Adamo, *J. Phys. Chem. A*, 2003, **107**, 11182.
35 C. Daul, E. J. Baerends and P. Vernooijs, *Inorg. Chem.*, 1994, **33**, 3538; S. R. Stoyanov, J. M. Villegas and D. P. Rillema, *Inorg. Chem.*, 2002, **41**, 2941; M.-F. Charlot, Y. Pellegrin, A. Quaranta, W. Leibl and A. Aukauloo, *Chem.–Eur. J.*, 2006, **12**, 796.
36 X. Zhou, A.-M. Ren and J.-K. Feng, *J. Organomet. Chem.*, 2005, **690**, 338.
37 A. B. P. Lever, *Compr. Coord. Chem. II*, 2003, 251, and references therein.
38 S. C. Rasmussen, S. E. Ronco, D. A. Mlsna, M. A. Billadeau, W. T. Pennington, J. W. Kolis and J. D. Petersen, *Inorg. Chem.*, 1995, **34**, 821; P. A. Adcock, F. R. Keene, R. S. Smythe and M. R. Snow, *Inorg. Chem.*, 1984, **23**, 2336; J. M. Calvert, R. H. Schmehl, B. P. Sullivan, J. S. Facci, T. J. Meyer and R. W. Murray, *Inorg. Chem.*, 1983, **22**, 2151; A. Ben Altabef, S. B. Ribotta de Gallo, M. E. Folquer and Nestor E. Katz, *Inorg. Chim. Acta*, 1991, **188**, 67; P. T. Gulyas, T. W. Hambley and P. A. Lay, *Aust. J. Chem.*, 1996, **49**, 527.
39 M. N. Golovin, Md. M. Rahman, J. E. Belmonte and W. P. Giering, *Organometallics*, 1985, **4**, 1981.
40 A. Altomare, M. C. Burla, M. Camalli, G. Cascarano, C. Giacovazzo, A. Guagliardi and G. Polidori, *J. Appl. Crystallogr.*, 1994, **27**, 435.
41 G. M. Sheldrick, *SHELXL-97, Program for refinement of crystal structures*, University of Göttingen, Germany, 1997; G. M. Sheldrick, *SHELXS-97, Program for solution of crystal structures*, University of Göttingen, Germany, 1997.
42 L. Farrugia, *J. Appl. Crystallogr.*, 1999, **32**, 837.
43 P. W. Betteridge, J. R. Carruthers, R. I. Cooper, K. Prout and D. J. Watkin, *J. Appl. Crystallogr.*, 2003, **36**, 1487.
44 *International Tables for X-Ray Crystallography*, ed. J. A. Ibers and W. C. Hamilton, Kynoch Press, Birmingham, UK, 1974, vol. 4.
45 A. L. Spek, *Acta Crystallogr., Sect. A: Found. Crystallogr.*, 1990, **46**, C34.
46 L. J. Farrugia, *J. Appl. Crystallogr.*, 1997, **30**, 565.